THE INTERNATIONAL SPAD SENSOR WORKSHOP (ISSW) 2024

10-µm InGaAsP/InP SPADs for 1064 nm detection with 36% PDP and 118 ps timing jitter

Utku Karaca, Ekin Kizilkan, Claudio Bruschini, and Edoardo Charbon

04.06.2024

Ecole polytechnique fédérale de Lausanne

Outline

1. Introduction & Motivation

2. Design & Simulations

3. Experimental Results

4. Conclusion

Applications of 1064 nm Single-Photon Detectors

1. Time-gated (domain) Diffuse Correlation Spectroscopy

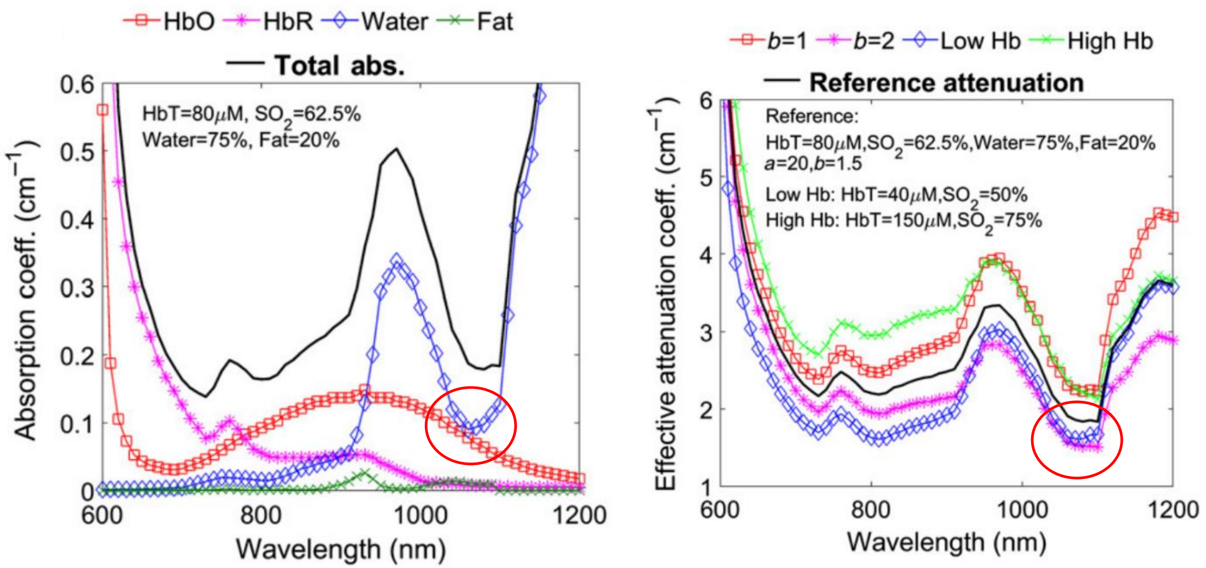

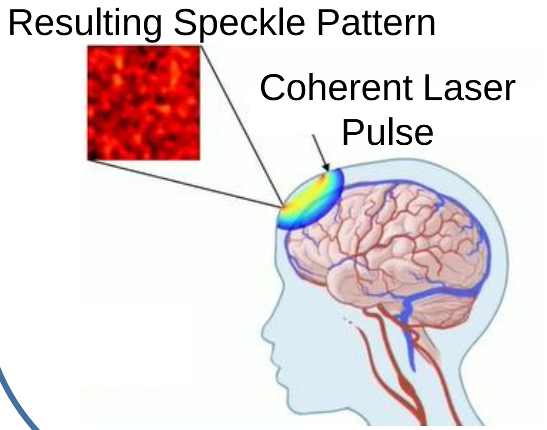

- Blood flow measurement in deep tissues
- Based on temporal light intensity fluctuations
- A minima in attenuation between 1050-1100 nm

Carb et al., J. Biomedical Optics (2020)

2. LiDAR for Space Measurements

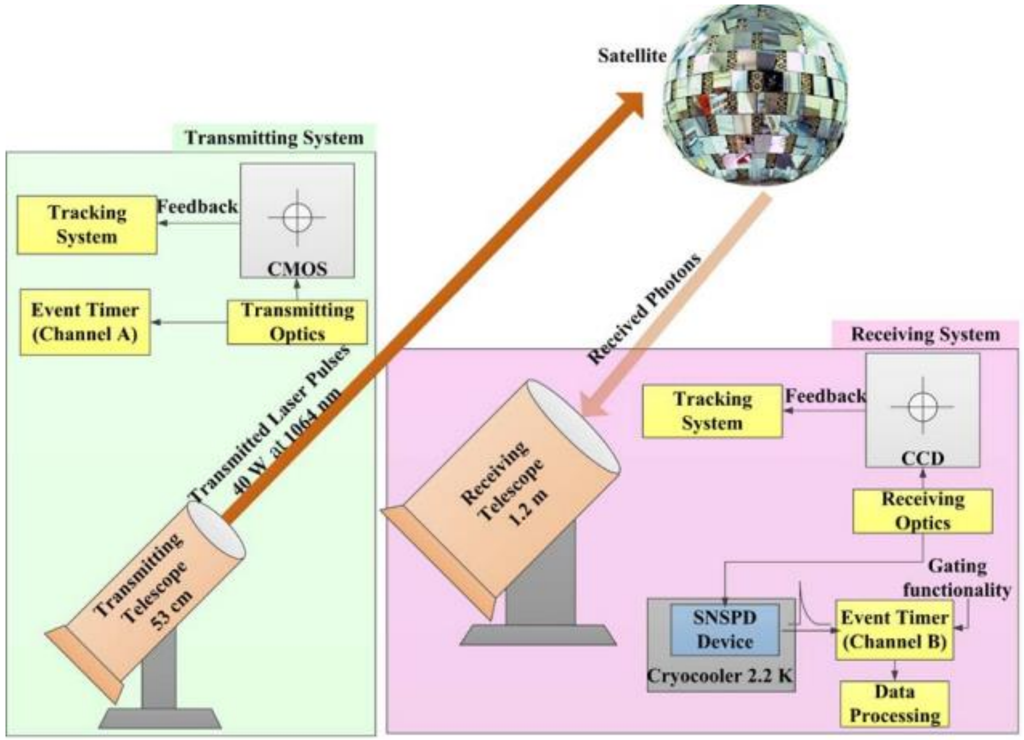

- Satellite orbit, space debris determination, etc.
- Solar radiation is 3× lower at 1064 nm compared to 532 nm ➔ increasing atmospheric propagation

Xue et al., Optics Letters (2016)

Detector of Choice

1. Superconducting nanowire single-photon detectors (SNPSDs)

- ✓ Reliable, usually preferred so far
- ✓ High detection efficiency, low dark count rates and timing jitter
- ○ **Need cryogenic temperatures and cryo pumps (expensive systems)**
- ○ **Not easily scalable**

2. InGaAs(P)/InP-based SPADs

- ✓ Variable bandgap ($In_xGa_{1-x}As_yP_{1-y}$)
- ✓ Detection between 900-1700 nm
- ✓ Direct bandgap (high absorption coefficient)
- ✓ Near room temperature operation possibility
- ✓ Scalable
- ○ **Technology is not very mature**
  - ➢ **Lower material qualities lead to high afterpulsing, limiting maximum operable frequency**

Objective

- **To design and fabricate InGaAsP/InP SPADs and SPAD arrays that:**
  - Are highly sensitive at 1064 nm wavelength
  - Provide low dark count rate (DCR) near room temperatures
  - Have low afterpulsing probability up to MHz operation
  - Have low timing jitter (< 200 ps) for the mentioned time-resolved application

Outline

1. Introduction & Motivation

2. Design & Simulations

3. Experimental Results

4. Conclusion

InGaAsP/InP SPAD Design Targeting 1064 nm

- Separate absorption-charge-multiplication (SACM) structure
- Based on hole multiplication
- InGaAsP absorber has a 1.1 µm cutoff wavelength and a 1 µm thickness (53% photon absorption).
- Charge layer doping ensures complete depletion of the absorber before the avalanche breakdown.

Planar (Double Zinc Diffusion) ***Both FSI and BSI compatible***

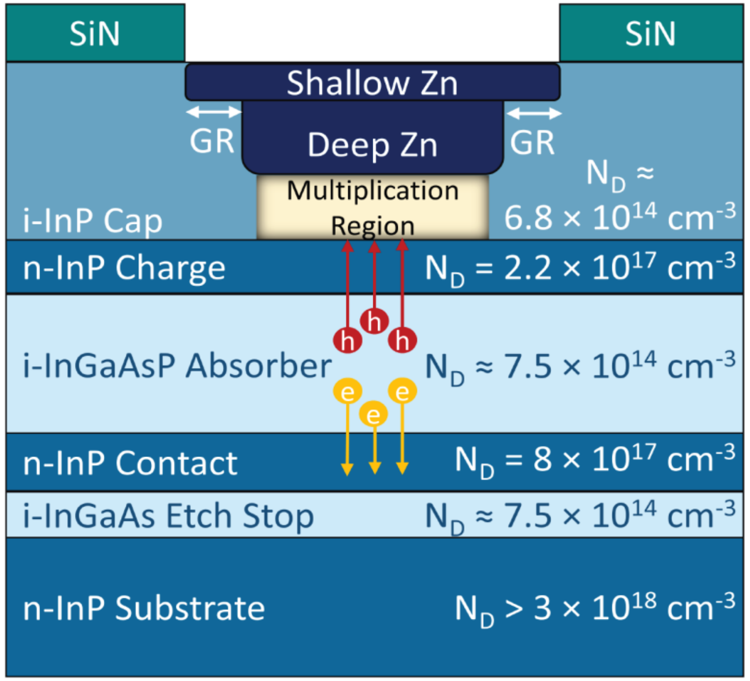

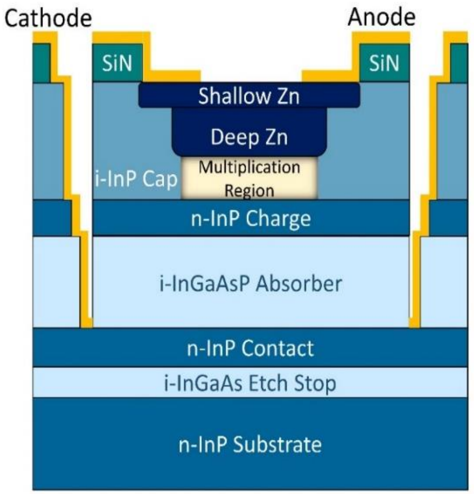

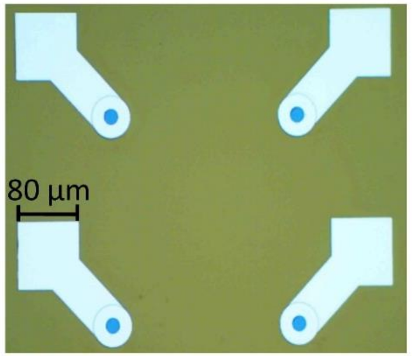

TCAD Simulations

- SPADs with a 10 μm active diameter and 2.5 μm GRs
- The curvatures of the Zn diffusions ➔ Error function
- Multiplication region thicknesses ➔ 1.5 μm, 1 μm, and 0.75 μm
- The Zn depth difference ➔ 0.5 μm

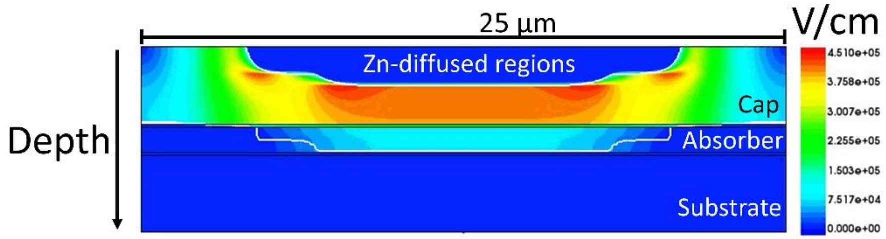

Simulated Electric Field Profile

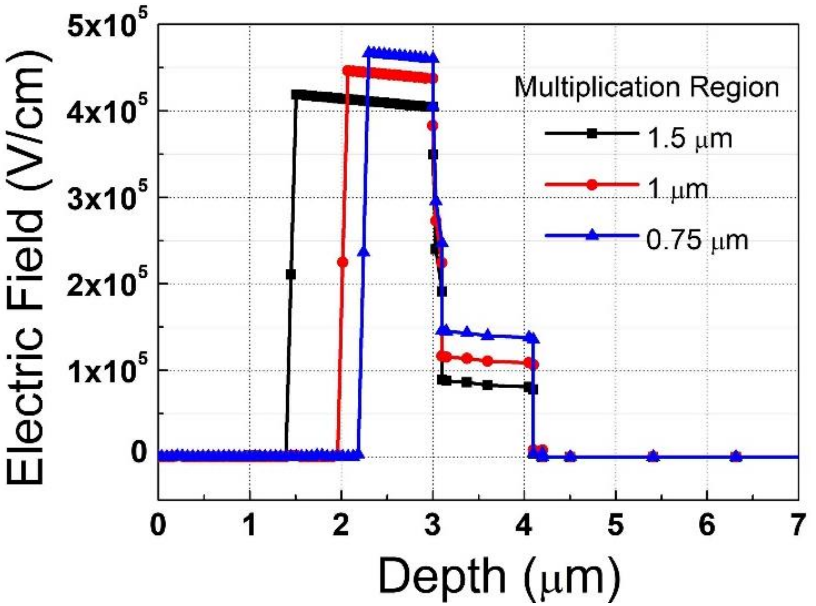

Simulated Electric Field Magnitudes

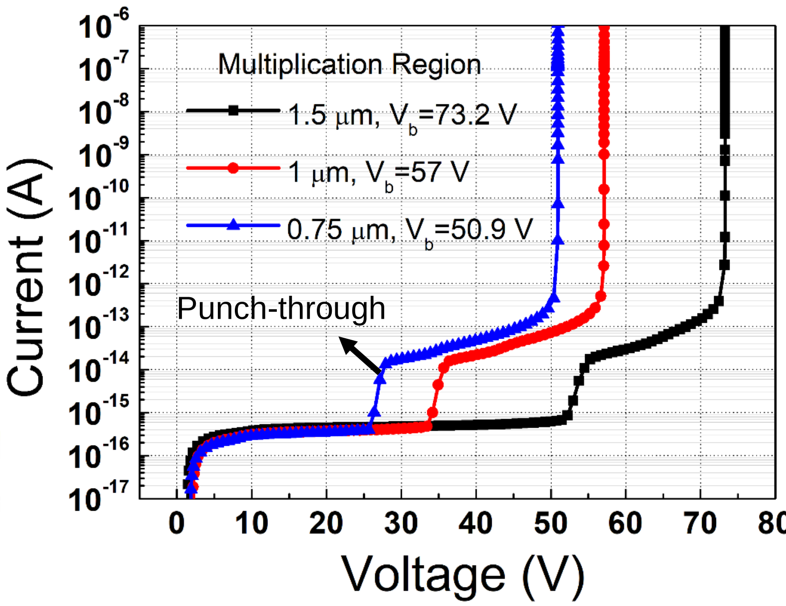

Simulated I-V Curves

TCAD Simulations

- Hole breakdown probability simulations indicate that:
  a) Edge effects are still present.
  b) More uniform photo-response while increasing V_{ex}

Deep Zn diffusion 1.5 µm, Shallow Zn diffusion 1 µm

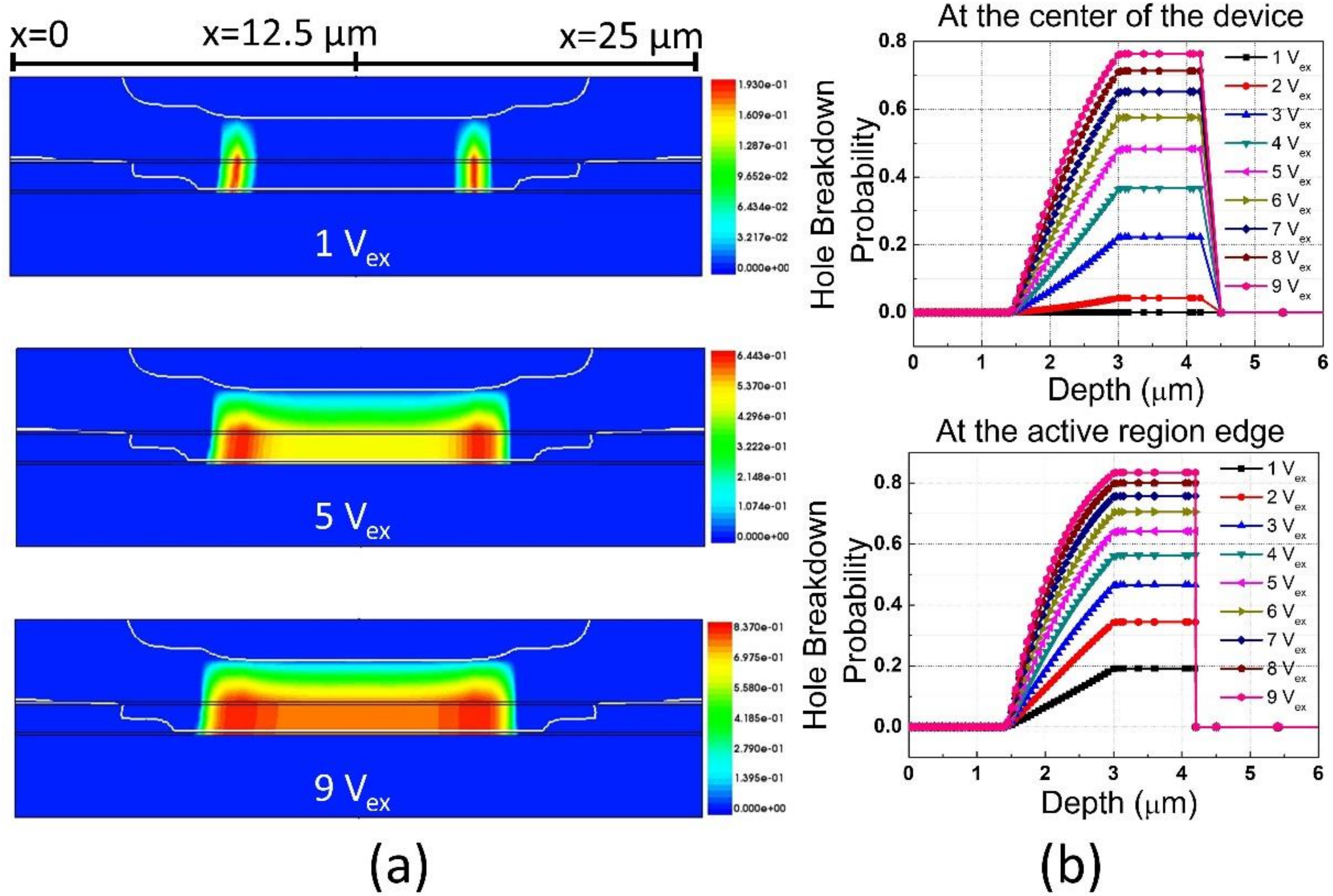

Outline

1. Introduction & Motivation
2. Design & Simulations
3. Experimental Results
4. Conclusion

SEM Analysis

- The obtained multiplication region thicknesses after the fabrication:

  ➔ 1.5 μm

  ➔ 1.3 μm

  ➔ 0.75 μm

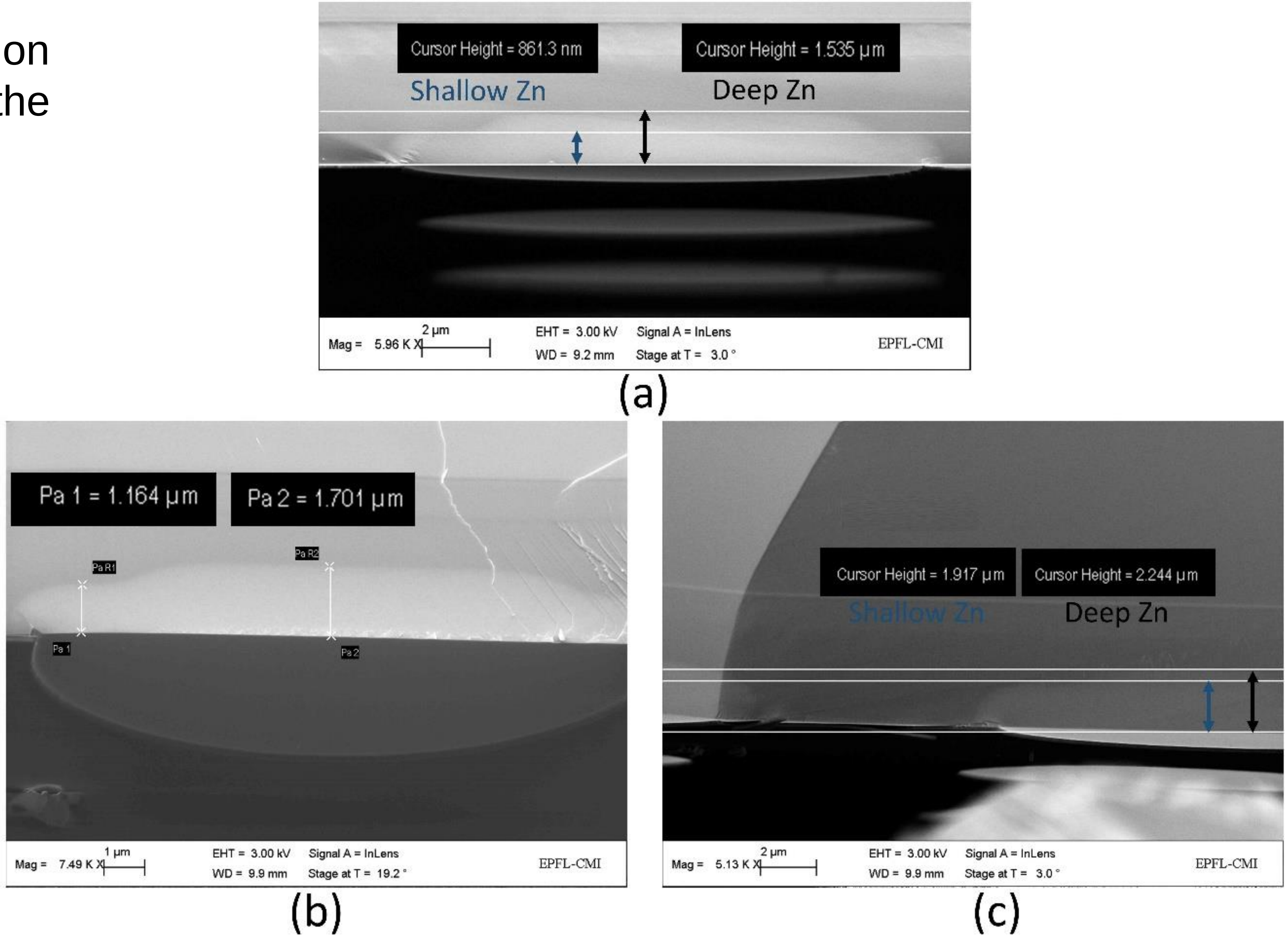

(a) (b) (c)

I-V Measurements

- Avalanche breakdown voltage increases with an increase in:
  - the multiplication region thickness due to the lower electric field confined ➔ lower avalanche breakdown probability
  - in the device diameter ➔ a larger mask opening results in shallower Zn diffusion
- Punch-through voltages occur far below the avalanche breakdown, indicating complete absorber depletion.

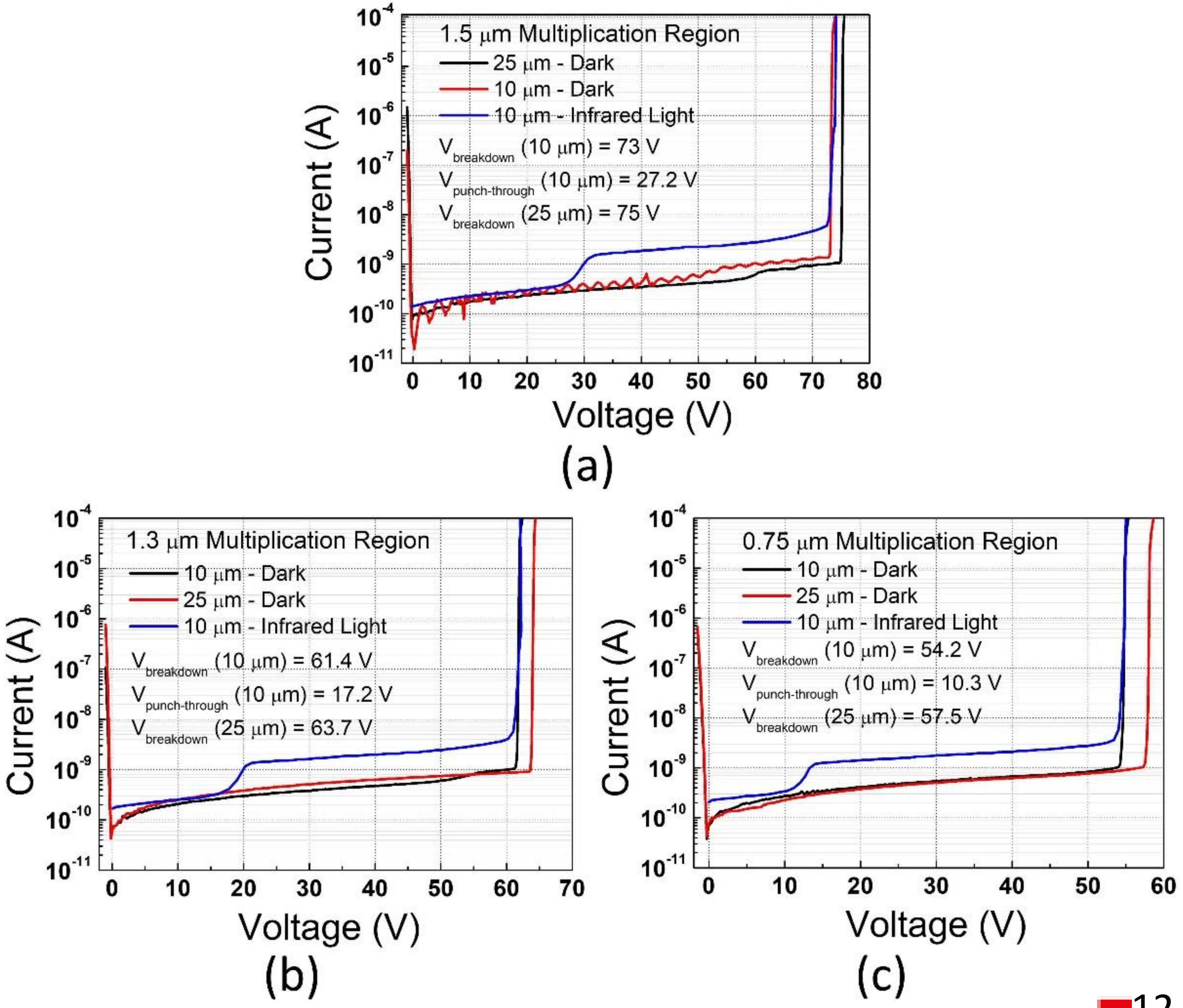

Gating Frequency Sweep Analysis

- Gating frequency sweep at 5 V_{ex} with 100 ns gate-on time showed that:
  a) At room temperature, up to 500 kHz (2 μs) gating with low APP can be achieved.
  b) At 225K, the maximum operable frequency is around 100 kHz due to longer carrier lifetimes.

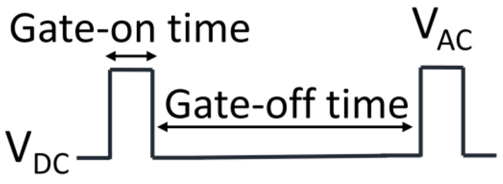

(a)

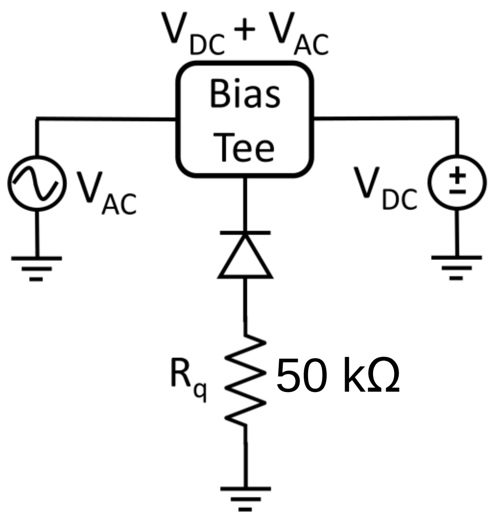

(b)

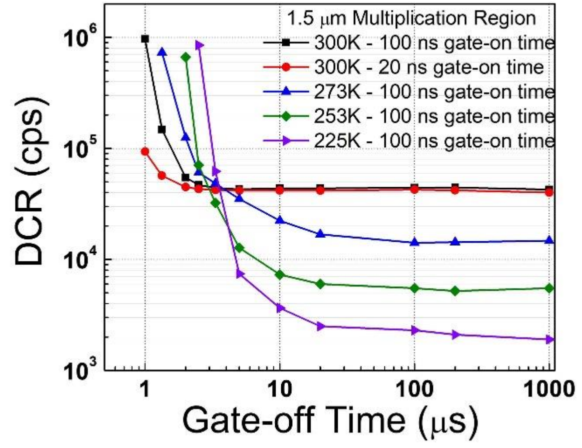

(a)

$$DCR_{gated\ mode} = \frac{C_{dark}}{f \times t_{on}}$$

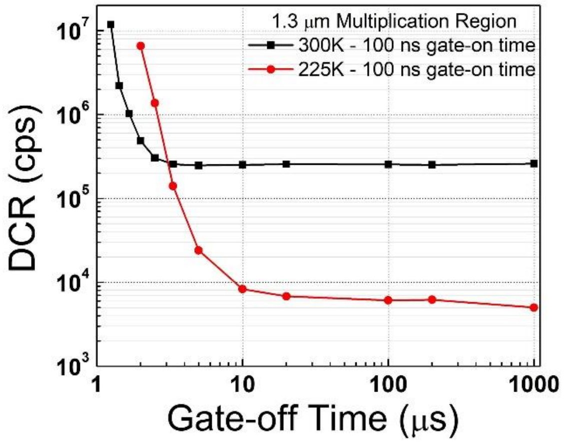

(b)

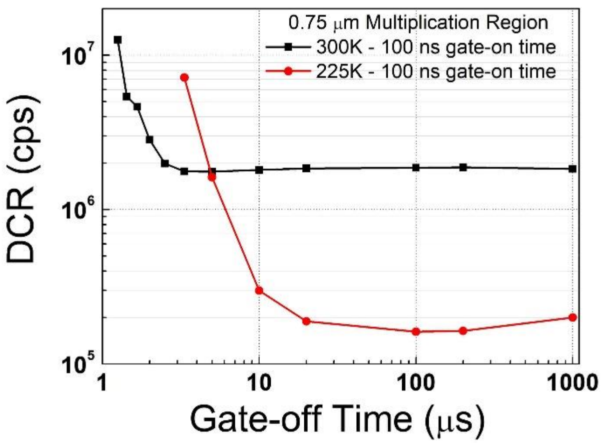

(c)

Dark Count Rate Measurements

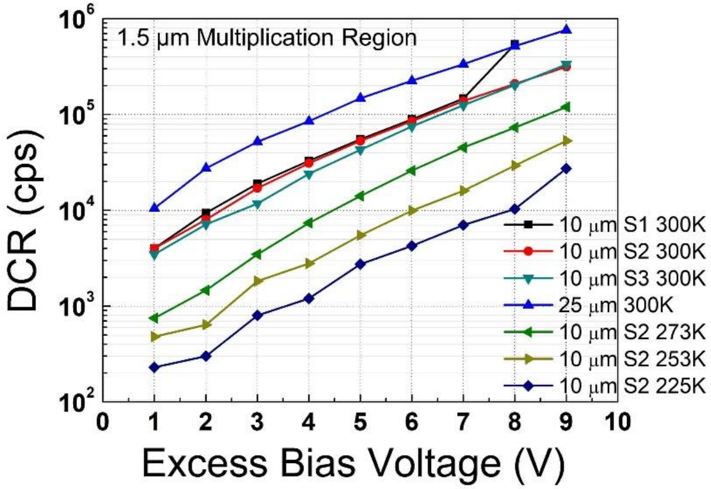

(a)

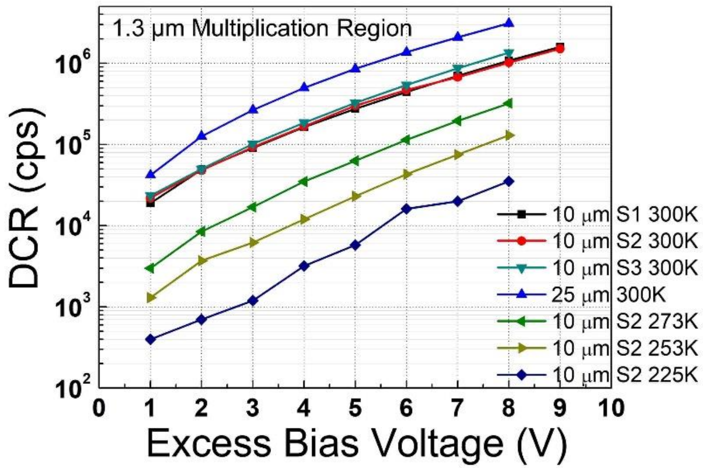

(b)

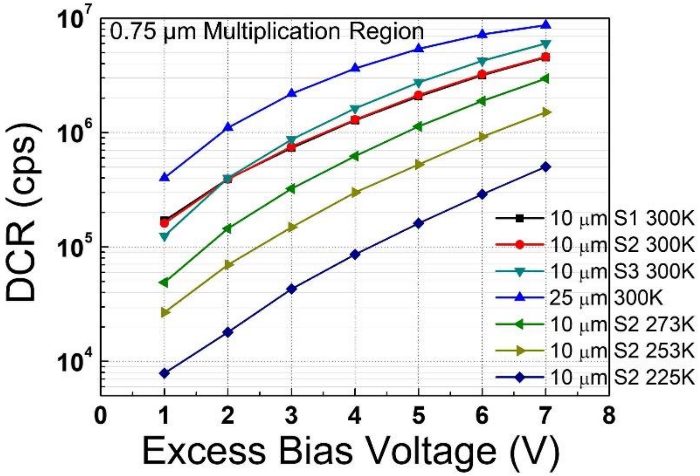

(c)

10 kHz frequency and 100 ns gate-on time in 10 µm diameter SPADs

DCR (cps) at 5 V_{ex}	1.5 µm	1.3 µm	0.75 µm
300K	53k	302k	2130k
273K	14.1k	40k	1040k
253K	5.5k	22k	510k
225K	2.75k	4k	180k

- DCR increases with reduced multiplication region thickness due to higher tunneling in InP.

Active Area Scanning Measurements

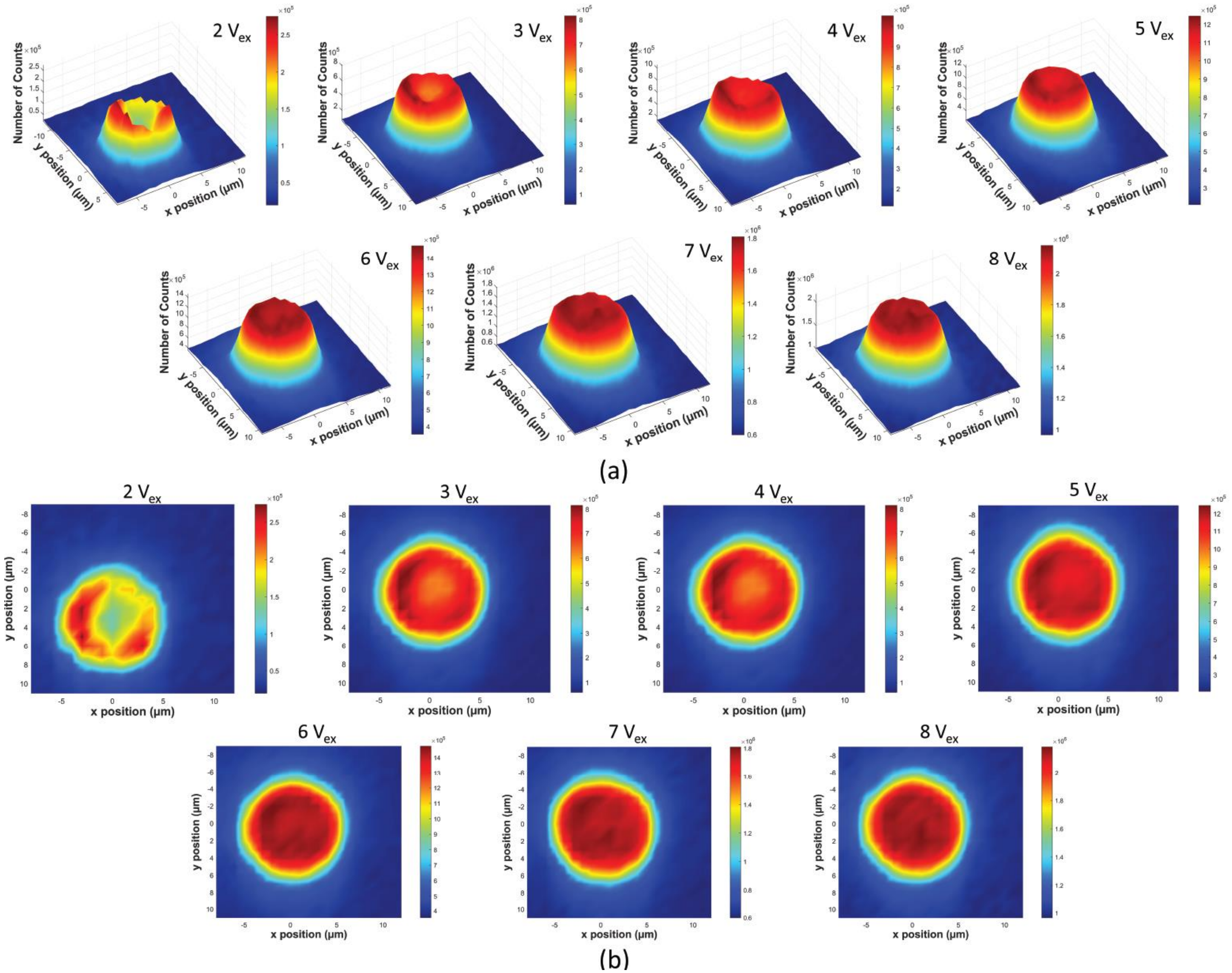

- Active area scanning at 1060 nm with a focused 1 μm laser beam from the backside showed that:

  a) The edge effects are present at low V_{ex}.

  b) The device response becomes uniform starting from 5 V_{ex}.

Photon Detection Probability Measurements

BSI SPADs

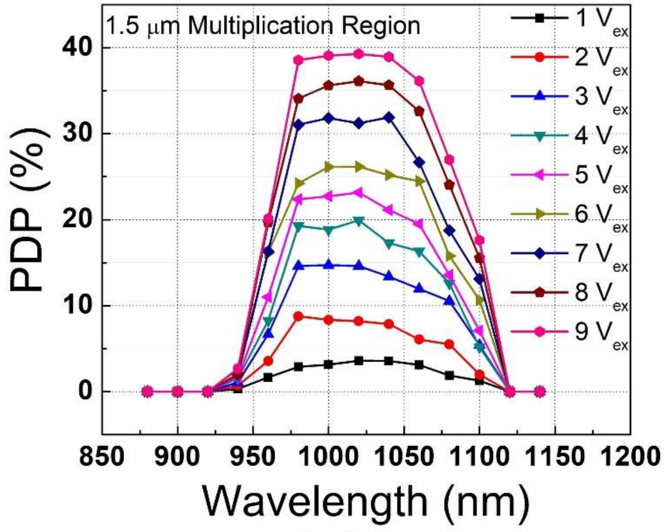

(a)

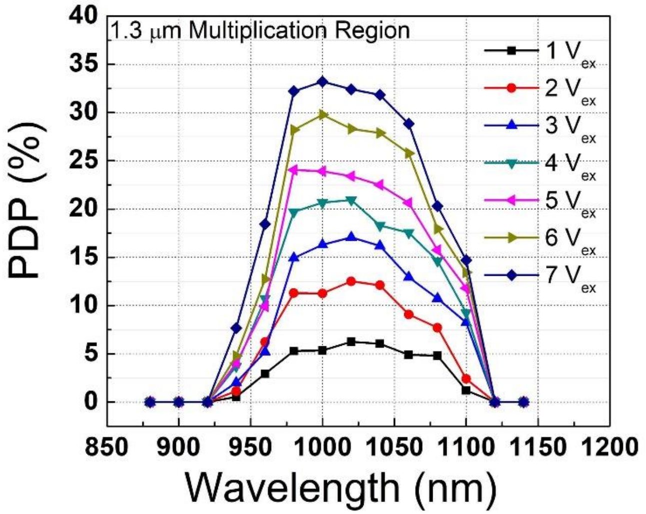

(b)

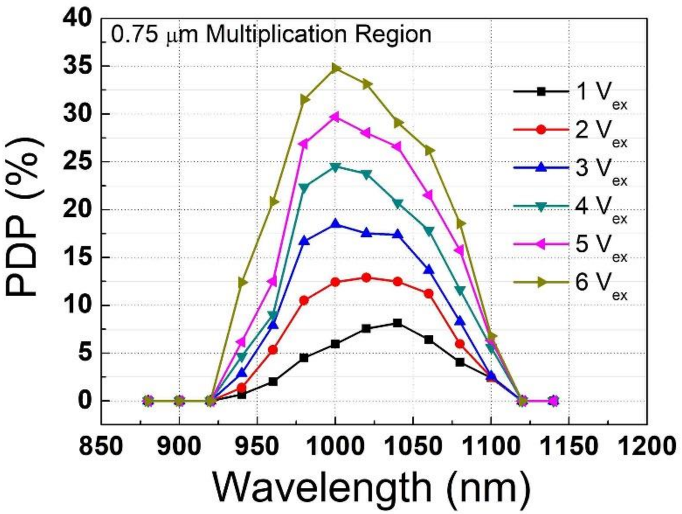

(c)

- The PDPs at 1060 nm and 5 V_{ex}
  1.5 μm ➔ 19.5%
  1.3 μm ➔ 20.4%
  0.75 μm ➔ 21.5%

- A high PDP of 36% at 9 V_{ex} was achieved in the SPAD with a 1.5 μm multiplication at the same wavelength.

$$PDP_{\text{gated mode}} = \frac{1}{\mu} ln \frac{1 - C_{\text{dark}}/f}{1 - C_{\text{total}}/f}$$

Measured with monochromator setup
μ: Mean number of photons per gate pulse
f: Gating frequency
C_{dark}: Count rate under dark
C_{total}: Count rate under illumination

Timing Jitter Measurements

- The timing jitters were calculated as 118.4 ps, 110 ps, and 84 ps FWHM at 5 V_{ex} for a 1.5 μm, 1.3 μm, and 0.75 μm multiplication region thickness, respectively, after the deconvolution.

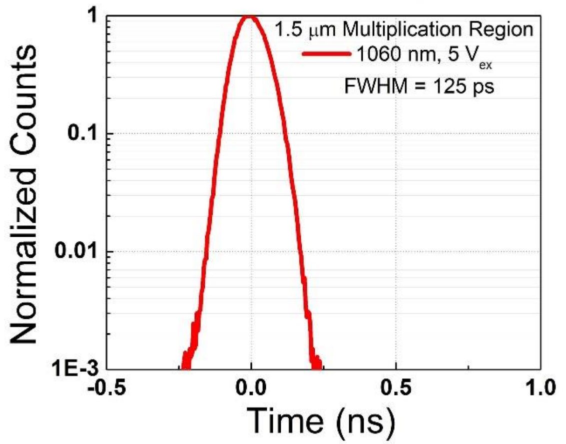

(a)

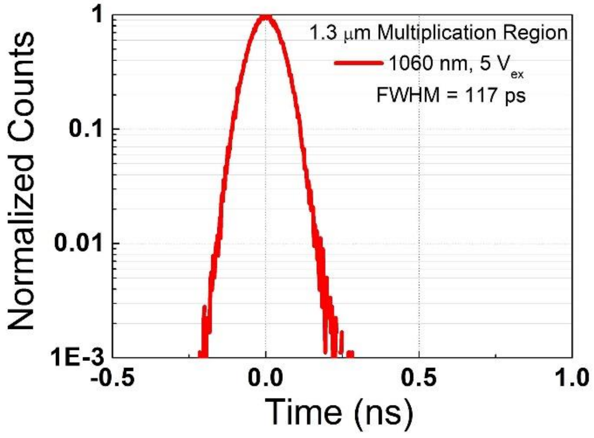

(b)

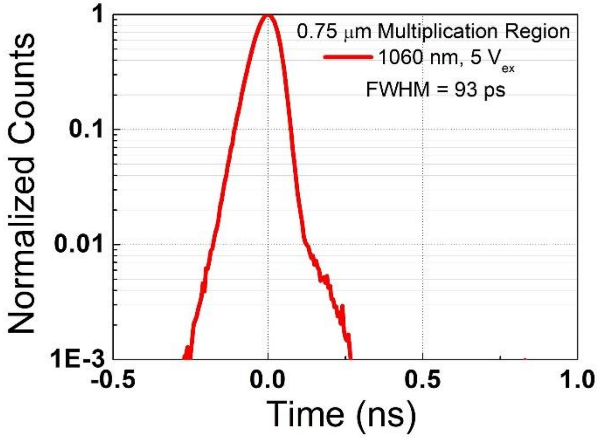

(c)

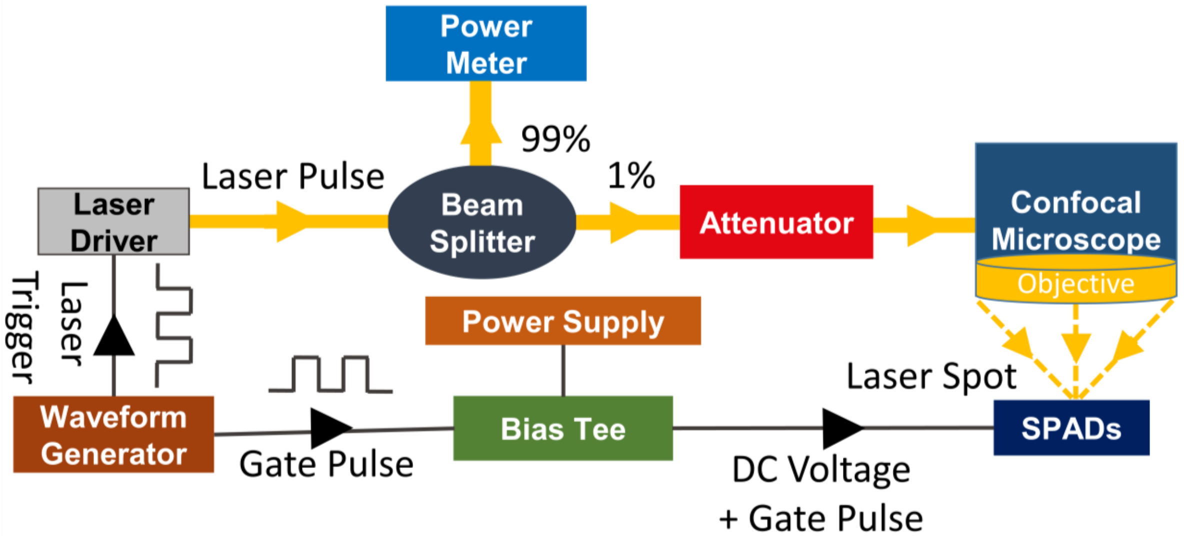

The laser was synchronized with the SPAD through the waveform generator operating at 10 kHz. The beam was focused at the center of the device.

Afterpulsing Probability Measurements

- Based on measuring inter-avalanche time
- For a 10 µm device with a 1.5 µm multiplication region and at 5 V_{ex}:
    a) The APP was 11.1% and 5.8% at 300K for 500 kHz and 200 kHz gating, respectively.
    b) The APP is increased to 12.8% and 33.5% at 273K and 253K, respectively, at 200 kHz.

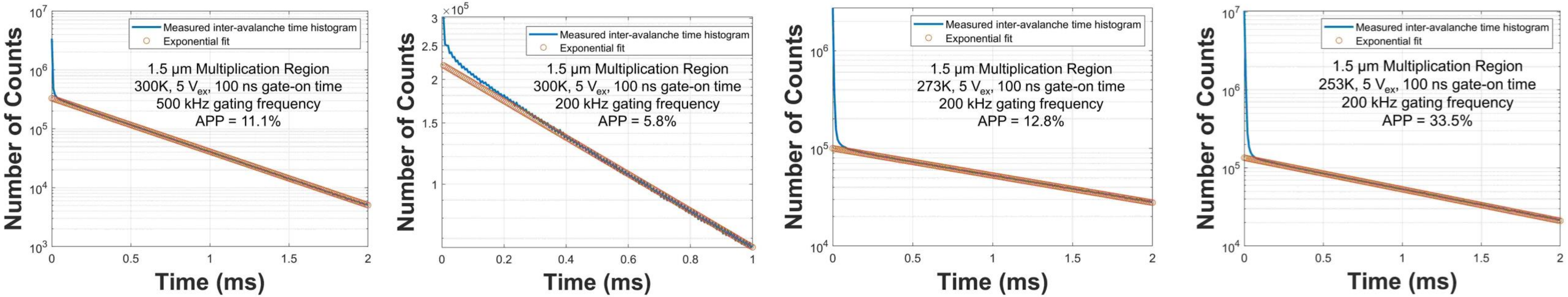

(a) (b) (c) (d)

Comparison with the state-of-the-art

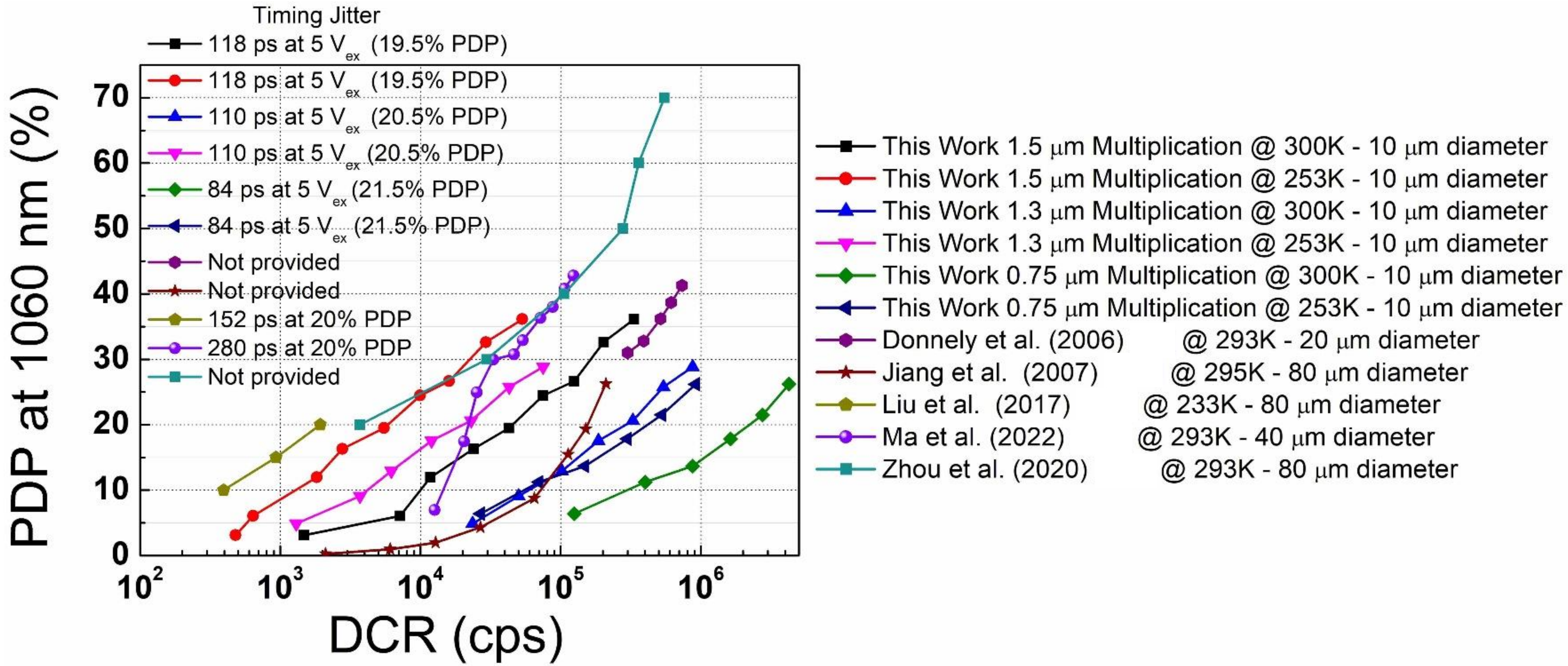

All references used FSI mode with a back-reflector metal. The presented SPADs were measured with BSI without a reflector on the front side.

Towards Arrays and 3D Integration of InGaAs(P) SPADs

- Demonstration of the scalability and integration of InGaAs(P)/InP SPADs with Si ROICs

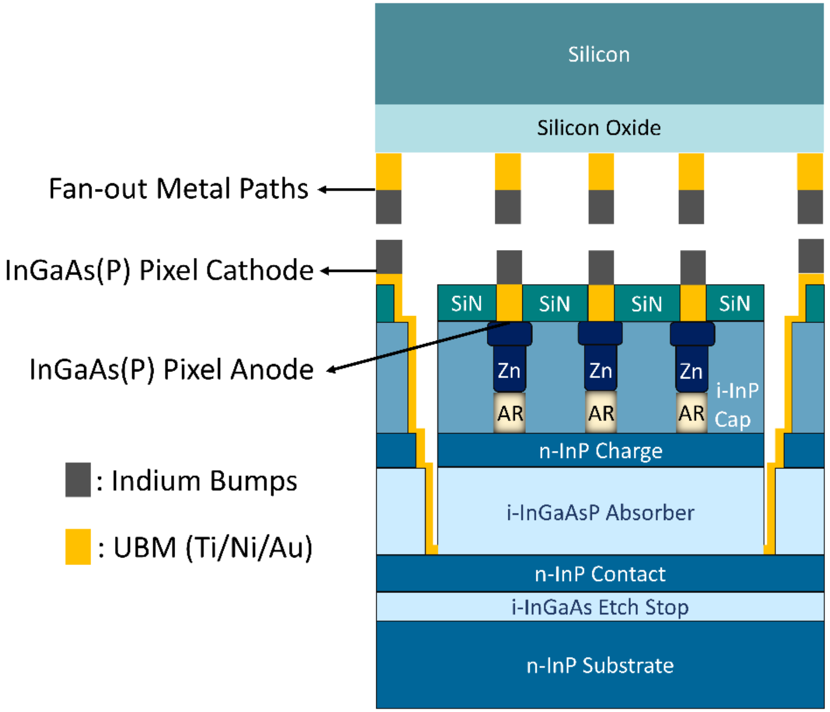

A Scheme of 3D Integration

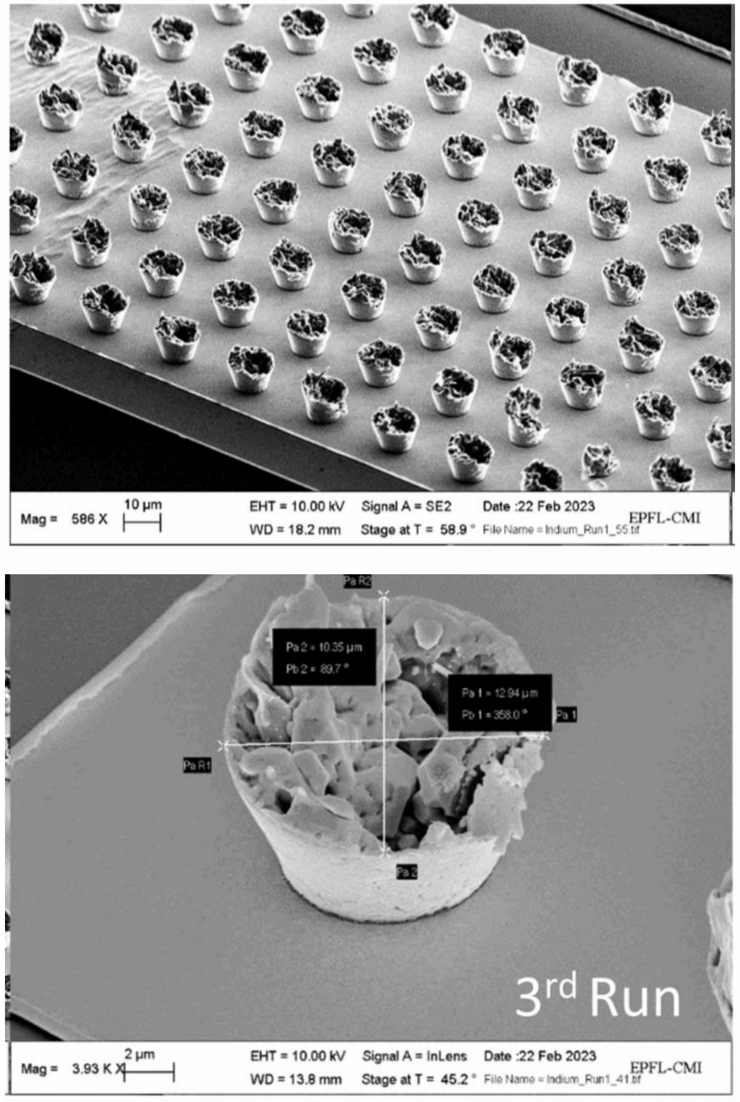

Indium Bump Development

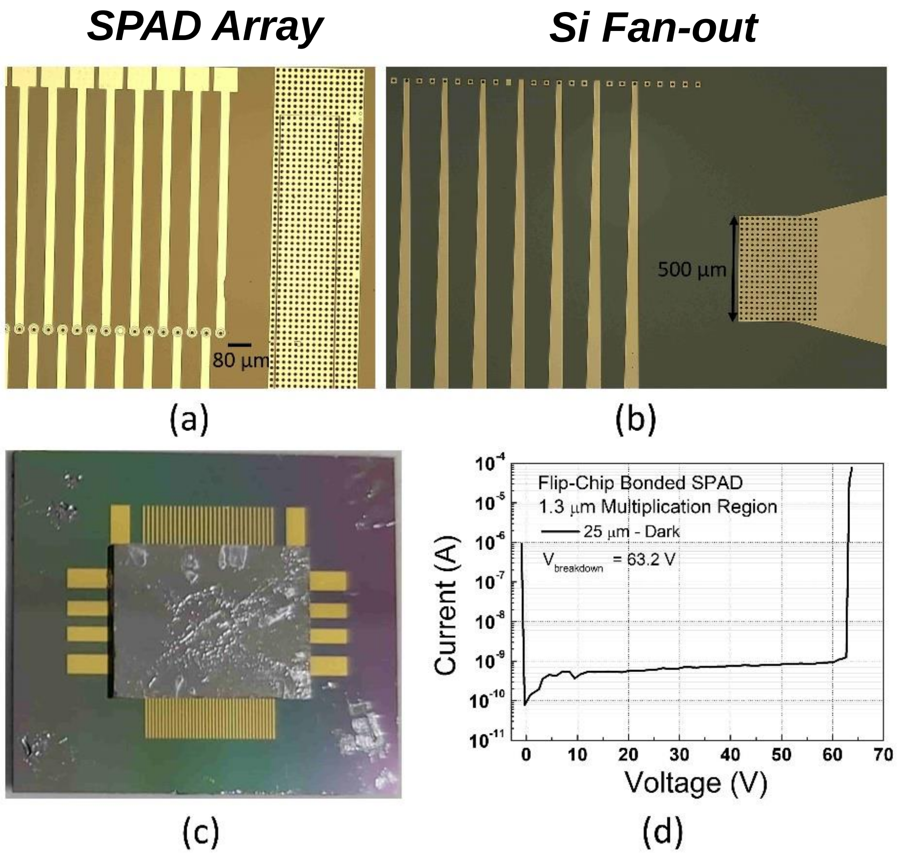

Flip-chip Bonding 1x128 InGaAsP SPAD Array with Developed Si Fan-outs

Conclusion

- A family of InGaAsP/InP SPADs targeting 1064 nm wavelength detection was fabricated and characterized.

- A 10-μm device with a 1.5 μm multiplication region can achieve 53 kcps and 118 ps timing jitter at 5 V_{ex}, 36% PDP at 9 V_{ex}.

- The afterpulsing of this device was 11.1% at 500 kHz, 300K, and 5 V_{ex}.

- Better jitter and PDP can be achieved with a smaller multiplication region thickness, at the expense of increased noise.

Thank you for your attention!

Questions?

Utku Karaca, Ekin Kizilkan, Claudio Bruschini, and Edoardo Charbon

04.06.2024

Ecole polytechnique fédérale de Lausanne